3. Carrier determination and frequency response of H_2 gas sensors based on dipyridyldiketopyrrolopyrroles

Introduction

In Chapter 2, details are given on the high-performance H_2 gas sensor [1] utilizing a high proton affinity of 1,4-diketo-3,6-bis-(4'-pyridyl)-pyrrolo-[3,4-*c*]-pyrrole (DPPP: Fig. 1) known as a red pigment [2]. The present sensor is based upon the accidental finding that exhibits a drastic reduction of the electrical resistivity in DPPP by five orders of magnitude due to protonation at the N atom of the pyridyl ring [3]. Fig. 2 illustrates the structure of the sensor together with our proposed operation principle. Our sensor device features a direct sputtering of Pd onto an interdigital electrode in the form of islands as shown in Fig. 2(b), followed by application of an extremely thin layer of DPPP under high vacuum (thickness: about 300-400 Å). As shown in Fig. 2(b), H_2 is first adsorbed on the surface of DPPP and diffuses into the bulk where H_2 encounters sputtered Pd. Then, H_2 can be dissociated into hydrogen atoms: H_2 (ads) $\rightarrow$ H (ads) + H (ads). At this moment, the N atom of the pyridyl ring of DPPP (strong proton acceptor) captures the proton, releasing an electron. In order to verify the present operation principle, it is crucial to show that the charge carriers are electrons in the present sensor. In this connection, an attempt was made to determine charge carrier of DPPP, its protonated species as well as the H_2 gas sensor by means of a thermoelectric power method based on the Seebeck effect.

The second part of the present chapter deals with the frequency response of the H_2 gas sensor studied with an intention of maximizing the sensor sensitivity. Under the operation of direct current (DC) as described in our previous paper [1], the electrical

contacts between DPPP and ITO are found to exert a profound influence on the sensor performance. When the ohmic contacts are formed, charge carriers will not accumulate at the “metal/semiconductor” interface and thus the electrons can flow freely without any obstacle. However, this is often not the case and the flow of charge carriers can be blocked, to some extent, with elapse of time due to space charges formed at the interface [1]. For this reason, a trial was made in the present investigation to drive the H_2 gas sensor with an alternating electric current (AC) in order to obviate possible problems associated with electrodes. To do this, it is indispensable to study the frequency response of the H_2 gas sensor.

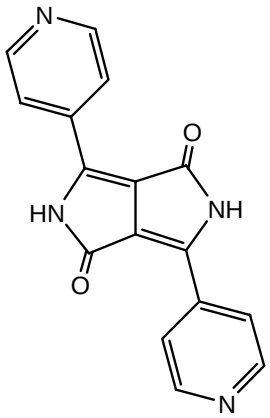

Fig. 1 Molecular conformation of DPPP.

Experiment

Seebeck coefficient and its experimental setup

In general, carrier determination in highly resistive materials is not an easy task because the number of charge carriers is quite small. Organic pigments such as DPPP falls in this category that has a resistivity of about 10^{11} Ωcm. For these materials, a thermoelectric power method based on the Seebeck effect is often quite helpful [4]. The thermoelectric power appears between hot and cold ends of the material. At the hot end,

electrons (or holes) will be excited to higher energies. Then, the higher-energy electrons (or holes) at the hot end are able to lower energies by diffusing to the cold end. Thus, the cold end becomes negatively (or positively) charged while the hot end positively (or negatively) charged, inducing a voltage along the direction of the temperature gradient.

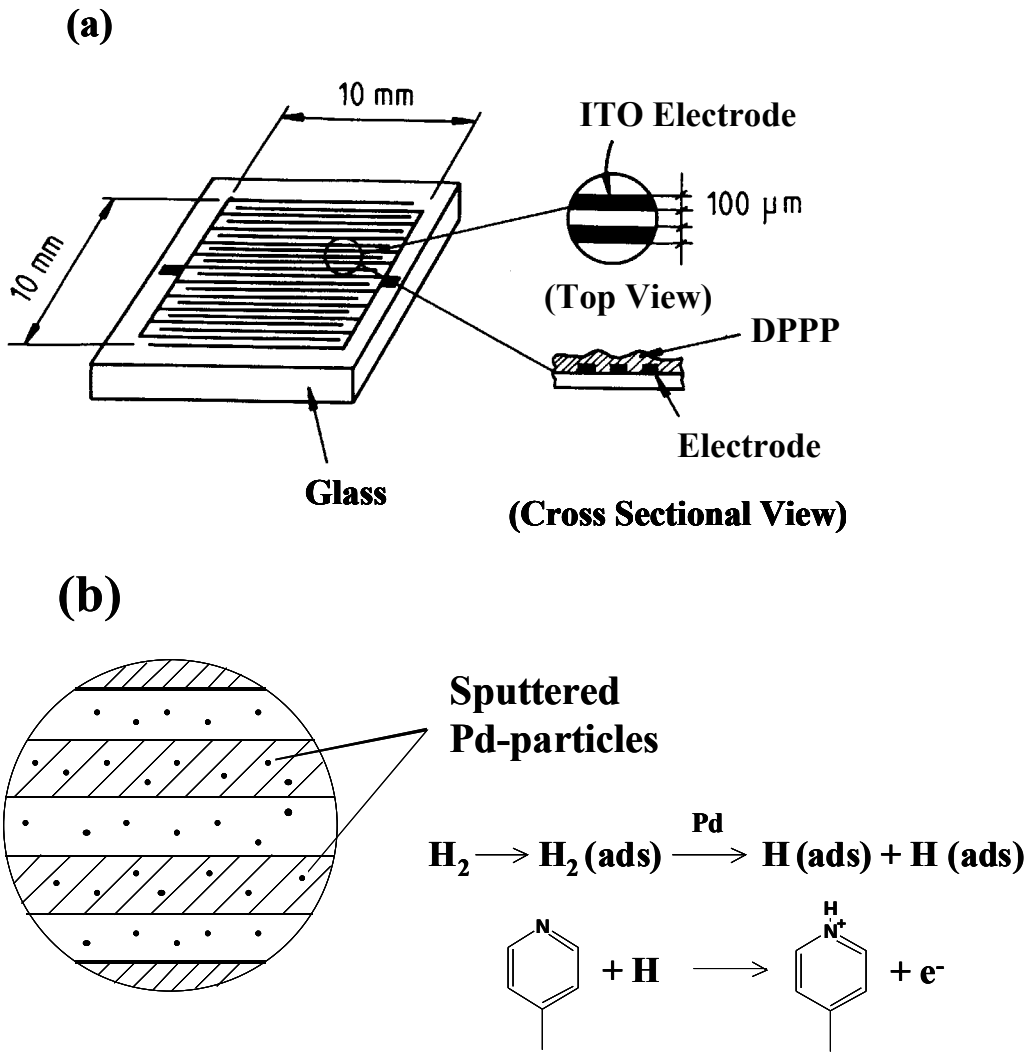

Fig. 2 Structure of the H_2 gas sensor: (a) interdigital electrodes and (b) magnified Pd-sputtered electrodes.

Fig. 3 shows the experimental setup for measurements of the Seebeck coefficient. A small spring contact is attached on top of the soldering iron for the sake of especially

soft contact with DPPP layers. The temperature of the soldering iron was maintained at 100 °C.

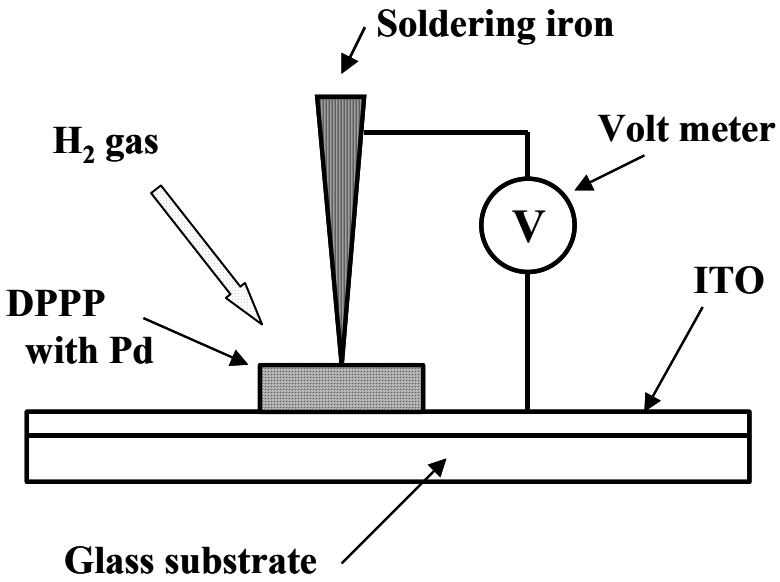

Fig. 3 Experimental setup for measurements of the Seebeck coefficient.

Samples used for measurements of the Seebeck coefficient

Three kinds of samples were prepared: evaporated DPPP, evaporated/protonated DPPP (which behaves as a model substance of the H_2 gas sensor) and the H_2 gas sensor based on DPPP. DPPP was deposited under high vacuum onto an ITO/glass-substrate (ITO: Indium-Tin-Oxide) to the thickness of about 1200 Å (Equipment: Tokyo Vacuum Co. Ltd.: model EG240). Protonation was carried out by exposing a deposited DPPP to the vapor of nitric acid. The H_2 gas sensor used has a slightly different structure from the standard one shown in Fig. 2, because the standard cell structure is not appropriate for the present measurement. Pd was first slightly sputtered onto an ITO/glass-substrate in the form of an island (thickness: about 3 Å) (equipment: E-1030 Ion Sputter from Hitachi Corporation), followed by deposition of DPPP under high vacuum (thickness: about 1200 Å). The DPPP layer was intentionally made thicker by roughly 3-5 times in

order to facilitate the present measurement. The present sample was therefore less sensitive by about two-three orders of magnitude as compared with our standard sensor based on an interdigital electrode, as illustrated in Fig. 2.

Measuring circuit for the frequency response of H_2 gas sensors

Fig. 4 shows the measuring circuit for the frequency response. The H_2 gas sensor is pictured as composed of a resistance and a condenser in parallel. A load resistance of 1 kΩ was connected in series with the gas sensor. Frequency response was measured with a voltage of 14 V_{eff} (effective voltage) of the sine wave in the range between 10 and 2×10^5 Hz.

Preparation of H_2 gas sensors

The interdigital ITO-electrodes whose intervals are 50 and 100 μm were prepared by photolithographic technique. Then, Pd was directly applied onto the interdigital electrode by sputtering in the form of islands so as to avoid contacts between two electrodes. After that, a thin layer of DPPP (300-400 Å) was applied by vacuum evaporation.

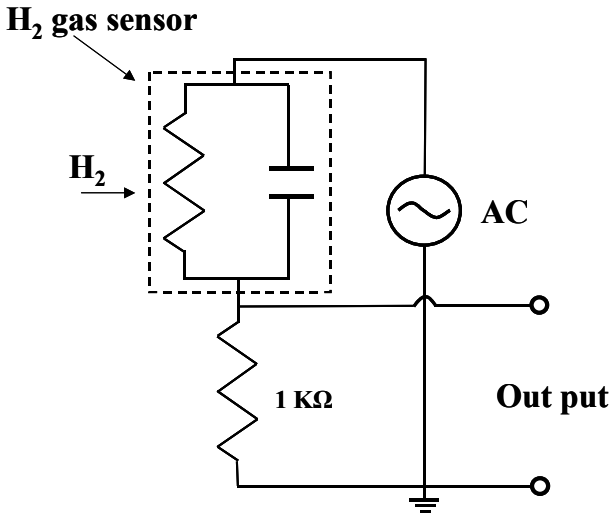

Fig. 4 AC electric circuit for measurements of the frequency response of the H_2 gas sensor.

Results and Discussion

Carrier determination

First of all, it should be remembered that the Seebeck potential in the present experiment is quite sensitive to the contact condition between the spring contact (attached to the soldering iron) and the sample surface. In spite of careful application of the spring contact on the sample surface, the spring can sometimes damage the thin layer of the test samples. Therefore, the magnitude of the potential is often scattered. Nevertheless, the sign of the potential remains quite reproducible.

Fig. 5 shows the thermoelectric power *vs* time for evaporated DPPP, evaporated/protonated DPPP as well as the H_2 gas sensor under 100 % H_2. As soon as the soldering iron comes into contact with the sample, a positive potential of about 0.2 mV appears at the hot end for evaporated DPPP. This indicates that DPPP conducts electrons. Similarly, evaporated/protonated DPPP exhibits an even larger potential of about 1 mV. Furthermore, upon introduction of H_2 gas, the H_2 gas sensor brings about a small positive potential of about 0.04 mV relative to DPPP. This evidently indicates that the charge carriers are due to electrons, just as in the case of evaporated DPPP and evaporated/protonated DPPP. The present result directly supports the operation principle of the H_2 gas sensor shown in Fig. 2(b).

Frequency response of the sensor

Since the H_2 gas sensor can be regarded as consisting of a resistance and a condenser as shown in Fig. 4, the current which flows through the circuit under H_2 includes two components: one is due to H_2 (*i.e.* real current) and the other is due to charge/discharge of the capacitance (*i.e.* displacement current). In order to separate these two components, the frequency response of the interdigital electrode with DPPP was also measured and

used as the reference.

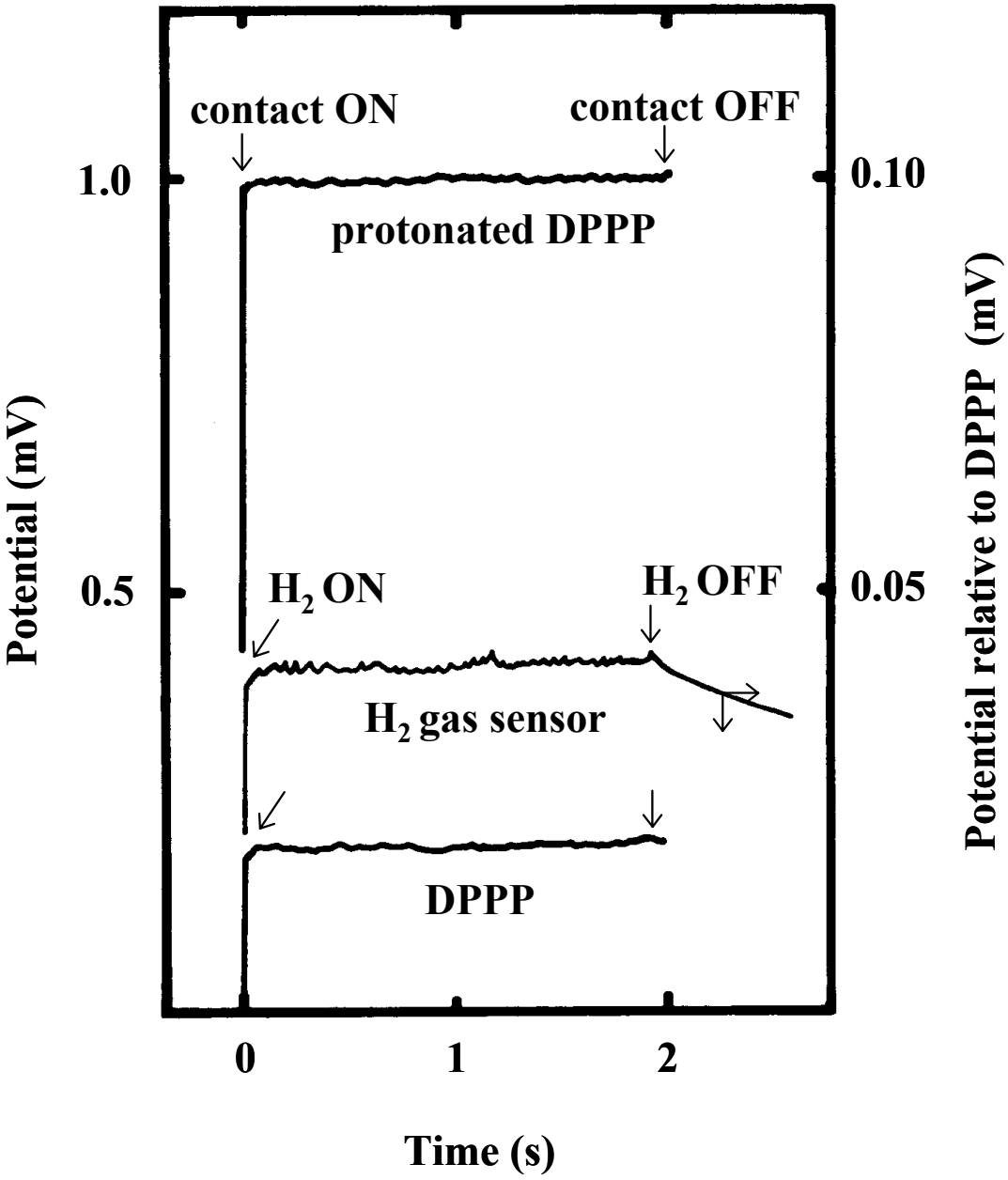

Fig. 5 Themoelectric power observed along the direction of the temperature radient: evaporated DPPP, evaporated/protonated DPPP and the H_2 gas sensor under 100 % H_2. The potential for the H_2 gas sensor is plotted relative to DPPP.

Fig. 6 shows the frequency response of the samples for electrode intervals of 50 and 100 μm in the presence or absence of 100 % H_2 gas. In both samples with 50 and 100 μm electrodes, the output voltage of the sensor is larger in the presence of H_2 in the frequency range from 10 to 5 kHz as compared with that of those in the absence of H_2. This difference is attributed to the real current (*i.e.* reaction current) due to H_2. The difference becomes larger as the frequency is lowered toward DC while smaller with higher frequencies. Then, no more difference is recognized in both samples above 5 and 10 kHz for the electrodes with 100 and 50 μm, respectively, where only displacement current prevails due to the condenser component of the sample. This indicates that the reaction rate for the detection of H_2 is too slow to follow the alternating electric field. These results prompt us to operate the sensor in the frequency region between 10 and 500 Hz.

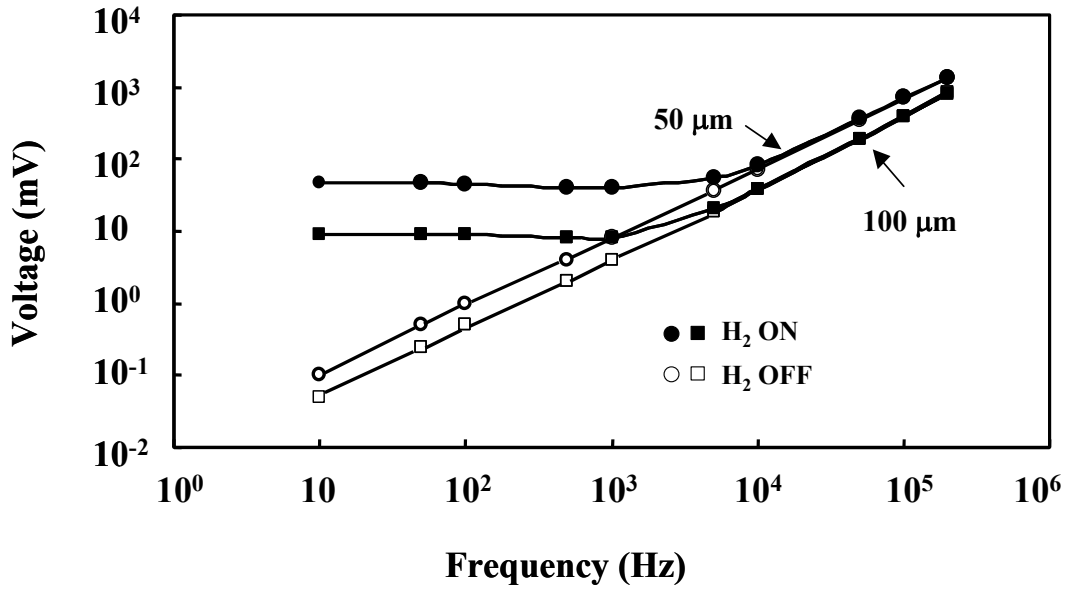

Fig. 6 Log-Log plot of the signal output *vs* frequency. Two types of electrode intervals were used: 50 and 100 μm. Measurements were made in the absence or presence of 100 % H_2.

Fig. 7 shows the build up of the signal output under the operation of DC and AC in the presence of H_2. AC voltages are expressed here in effective values. It is remarkable to note that the AC 30 V_{eff} gives a higher output than DC 30 V by a factor of 1.5. The output voltage is further enhanced by a factor of 1.75 with AC 60 V_{eff} as compared with that of DC 60 V. These results lead us to conclude that AC drive provides basically a better performance of the sensor by a factor of 1.5-1.75. The enhancement of the output signal can largely be attributed to the obviation of the polarization effect due to DC drive at the interface between electrode and DPPP.

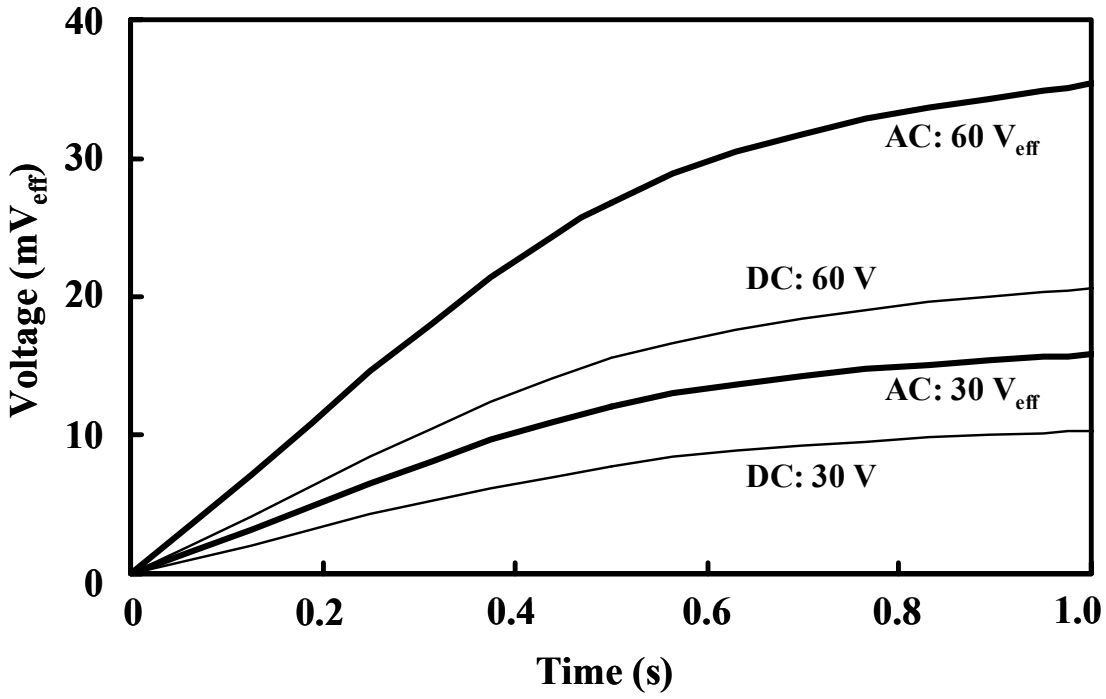

Fig. 7 Build-up of the sensor signal under 100 % H_2 with the operation of DC and AC. Cell structure: ITO/Pd/DPPP/ITO.

Conclusions

Carrier determination and frequency response of the H_2 sensors based on DPPP have been investigated. The following conclusions can be summarized.

1. The charge carriers are determined to be electrons for evaporated DPPP, evaporated/protonated DPPP and the H_2 sensors based on DPPP.
2. The H_2 gas sensor is found to enhance the output signal under AC operation by a factor of about 1.5-1.75 in the frequency range between 10 and 500 Hz, as compared with DC drive.

References

1. H. Takahashi and J. Mizuguchi, *J. Electrochem. Soc.* **152**, H69-H73 (2005) .
2. M. Herbst and K. Hunger, *Industrial Organic Pigments*, pp.550-553, VCH, Weinheim, (1993).
3. J. Mizuguchi, *Ber. Bunsenges. Phys. Chem.*, **97**, 684 (1993).
4. C. Kittel, *Introduction to Solid State Physics*, sixth edition, John Wiley & Sons, Inc. New York (1986).